A STUDY ON QUANTITATIVE ANALYSIS OF DENDRITIC SPINES FROM HIGH-RESOLUTION MICROSCOPIC IMAGES

A thesis

submitted in partial fulfilment of the requirement for the Degree of

Master of Technology in Computer Technology

of

Jadavpur University

By

Sneha Podder

Registration No.: 149860 of 2019-2020

Examination Roll No.: M6TCT22027

Under the Guidance of

Dr. Subhadip Basu

Department of Computer Science and Engineering

Jadavpur University, Kolkata-700032

2022

FACULTY OF ENGINEERING AND TECHNOLOGY

JADAVPUR UNIVERSITY

Certificate of Recommendation

This is to certify that the dissertation entitled "**A Study on Quantitative Analysis of Dendritic Spines from High-Resolution Microscopic Images**" has been carried out by Sneha Podder (University Registration No.: 149860 of 2019-2020, Examination Roll No.: M6TCT22027) under my guidance and supervision and be accepted in partial fulfilment of the requirement for the Degree of Master of Technology in Computer Technology. The research results presented in the thesis have not been included in any other paper submitted for the award of any degree in any other University or Institute.

……

Dr. Subhadip Basu (Thesis Supervisor)

Department of Computer Science and Engineering

Jadavpur University, Kolkata-32

Countersigned

…….

Prof. Nandini Mukhopadhyay

Head, Department of Computer Science and Engineering,

Jadavpur University, Kolkata-32.

…….

Prof. Chandan Mazumdar

Dean, Faculty of Engineering and Technology,

Jadavpur University, Kolkata-32.

FACULTY OF ENGINEERING AND TECHNOLOGY

JADAVPUR UNIVERSITY

Certificate of Approval

This is to certify that the thesis entitled "A Study on Quantitative Analysis of Dendritic Spines from High-Resolution Microscopic Images" is a bonafide record of work carried out by Sneha Podder in partial fulfilment of the requirements for the award of the Degree of Master of Technology in Computer Technology in the Department of Computer Science and Engineering, Jadavpur University during the period of July 2021 to August 2022. It is understood that by this approval, the undersigned does not necessarily endorse or approve any statement made, opinion expressed or conclusion drawn therein but approves the thesis only for the purpose it has been submitted.

……..

Signature of Examiner 1

Date:

……..

Signature of Examiner 2

Date:

FACULTY OF ENGINEERING AND TECHNOLOGY

JADAVPUR UNIVERSITY

Declaration of Originality and Compliance of Academic Ethics

I hereby declare that this thesis entitled "A Study on Quantitative Analysis of Dendritic Spines from High-Resolution Microscopic Images" contains a literature survey and original research work by the undersigned candidate as part of my Degree of Master of Technology in Computer Technology.

All information has been obtained and presented in accordance with academic rules and ethical conduct.

I also declare that, as required by these rules and conduct, I have fully cited and referenced all materials and results that are not original to this work.

Name: Sneha Podder

Registration No: 149860 of 2019-2020

Exam Roll No.: M6TCT22027

Thesis Title: "A Study on Quantitative Analysis of Dendritic Spines from High-Resolution Microscopic Images"

…..……..

Signature with Date

Acknowledgement

I would like to thank the holy trinity for helping me deploy all the right resources and shaping me into a better human being. I would like to express my deepest gratitude to my advisor, **Dr. Subhadip Basu**, Department of Computer Science and Engineering, Jadavpur University, for his admirable guidance, care, patience and for providing me with an excellent atmosphere for doing research. Our numerous scientific discussions and his many constructive comments have greatly improved this work.

Thank you to **Dr Jakub Wlodarczyk and Ewa Bączyńska,** Department of Molecular and Cellular Neurobiology, Nencki Institute of Experimental Biology, Warsaw, Poland, for providing the essential data for our research, without which we cannot test our method's efficiency.

Among the seniors, I am deeply grateful to **Mr Shauvik Paul and Mr Nirmal Das** for their guidance and supervision throughout the project. Without his enthusiasm, encouragement, support and endless optimism, this thesis would hardly have been continued.

Most importantly, none of this would have been possible without the love and support of my family. I thank my parents and in-laws, whose forbearance and whole-hearted support helped this endeavour succeed.

This thesis would not have been completed without the inspiration and support of several wonderful individuals. I appreciate all of them for being part of this journey and making this thesis possible.

……..

Sneha Podder

Registration No: 149860 of 2019-2020

Exam Roll No.: M6TCT22027

Department of Computer Science & Engineering, Jadavpur University

Contents

Chapter 1

Introduction

Spine morphology and distribution are important factors associated with numerous neurological disorders such as mental retardation and schizophrenia for spine morphological abnormalities. Therefore, the visualization and analysis of dendritic spines are critically important for research on synaptic plasticity. Dendritic spines are the postsynaptic morphological specializations that receive synaptic impulses.

It is widely believed that long-term synaptic plasticity is accompanied by structural changes in synapses, particularly at dendritic spines. In 1995, Michele Papa *et al.* [1] monitored development alternation in the dendritic spine in the primary culture of hippocampal neurons using Confocal Laser Scanning Microscopy (CLSM). They observed the morphological changes of neurons over four weeks. In 1996, a study [2] showed that the dendritic spine is a dynamic structure, highly responsive to changes in the ambient condition. Dendritic spines change shape and size, and their turnover rates decline with age. The complex mechanism behind memory creation and retention is assumed to incorporate synaptic plasticity in the hippocampus and cerebral cortex.

1.1 Dendritic Spine: relevance to brain activity and neuro diseases

Dendritic spines are the postsynaptic components of most excitatory synapses in the mammalian brain. Spines accumulate rapidly during early postnatal development and undergo a substantial loss as animals mature into adulthood. Dendritic spines are the key elements for information acquisition and retention; understanding how spines are formed and maintained,

particularly in the intact brain, will likely provide fundamental insights into how the brain possesses the extraordinary capacity to learn and remember.

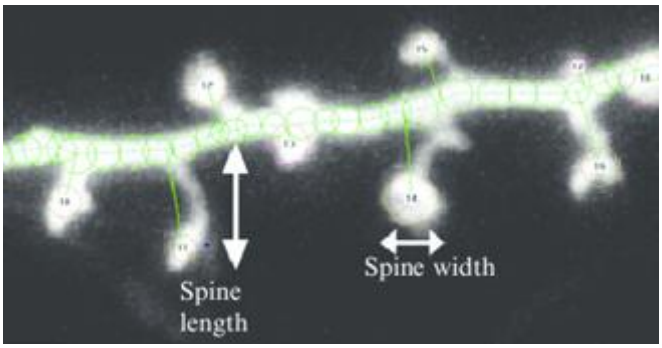

Figure 1.1: Sample image of Spine Morphology

Spine morphology has been related to a specific component of cognitive process, such as learning, i.e. accusation of information and memory creation, i.e. long-term information retention. The functional interplay between neuronal activity and different signalling pathways can induce new spine growth and affect spine maturation and stabilization/pruning, the processes that are essential for learning and memory [3]. Impaired spine dynamics can cause psychiatric and neurodevelopmental disorders.

Pathological conditions like Alzheimer's (AD), an age-related neurodegenerative disease, causes elderly death. AD symptoms are early memory deficits, followed by dementia, i.e. the gradual decline of cognitive and intellectual functions [4]. Poor spine density and abnormal spine morphology, including alteration of their shapes and smaller size, have been found in schizophrenic patients [5]. Mental retardation is associated with distorted spines, including headless or enlarged heads.

1.2 Dendritic Spine Classification

Spine morphology and stabilization are highly influenced by synaptic activity. Spine morphology has exhibited a high degree of plasticity in recent years. In developing tissue, such as organotypic slice cultures, shape changes in spines and reorganization of the postsynaptic density (PSD) occur within minutes [6]. Furthermore, several studies have shown that these and other changes can be induced by or are dependent on synaptic activation. Spines are classified into four classes: Stubby, Filopodia, Mushroom and Spine-head Protrusions. During the spinogenesis process, as the spine starts to develop, they build a long, thin-like form called a filopodium [7]. Filopodium is normally witnessed during development. This type of spine has a long neck and no head. Over time filopodia is replaced by a thin, i.e. spine with a long neck and small head, stubby, i.e. spines with no neck or short neck and relatively mature mushroom-shaped spines, i.e. spines with a long neck and large bulbous head [8]. Mushroom-shaped spines, considered to be mature spines, are typically more stable and have an enlarged spine head containing neurotransmitter receptors and a postsynaptic density (PSD), whereas filopodium is immature spines with a lack of synapses.

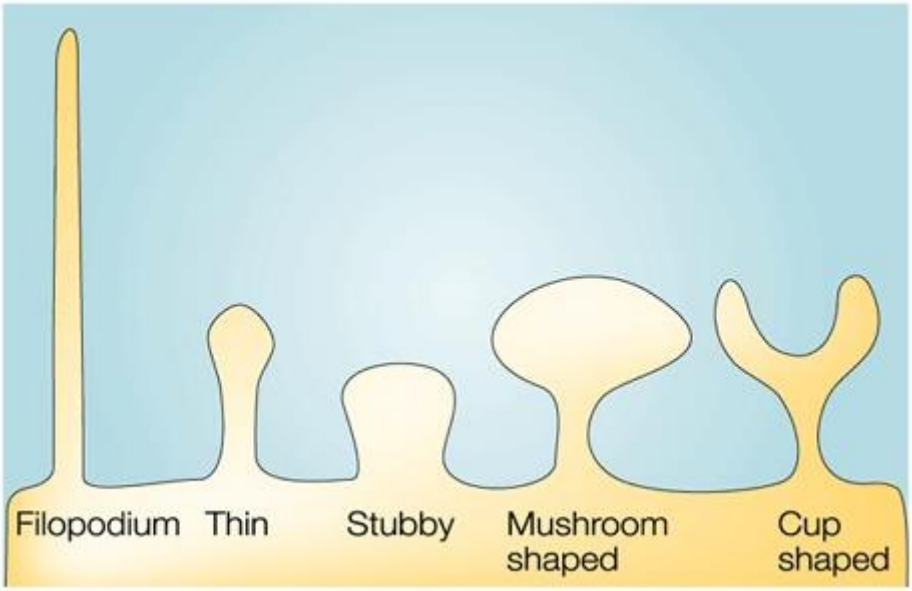

Figure 1.2. Different spine morphologies

(Image courtesy: site- Researchgate.net; link-

https://www.researchgate.net/figure/Morphological-classification-of-dendritic-spines_fig3_11622109)

1.3 Imaging Modalities

The advancement of biomedical imaging technologies allows the visualization of multi-dimensional data, revolutionarily impacting biomedical research. Bio-medical imaging measures physical parameters such as density, concentration, tissue properties, and surface area. There are many imaging tools, including innovative microscopy methods, ultrasound, computed technology (CT), Magnetic Resonance Imaging (MRI) and Positron Emission Tomography (PET). Super-resolution microscopy provides optical access to the intricate morphology of neurons in living brain tissue, resolving their finest structural details, which are critical for neuronal function. SpineJ is a semi-automatic ImageJ plugin that provides an intuitive and user-friendly graphical user interface, facilitating fast, accurate, and unbiased analysis of spine morphology[9].

However, dendritic spines feature nanoscale structural details, such as spine necks, which are functionally very important but cannot be properly resolved by conventional optical techniques like confocal and two-photon microscopy. Given this technical limitation, researchers have instead used calibrated fluorescence measurements to estimate spine size. The advancement of fluorescence microscopy has been a major step toward enhancing living cells study. It is possible to have an insight into cell structure and function using fluorescence microscopy.

Confocal microscopy is used to investigate cells' structural and morphological properties and differentiate between normal and odd cells for diagnosis. In confocal microscopy, optical or fluorescent properties of a specimen are measured by blocking all out-of-focus light using a small pinhole, i.e. only considering the light reflected from the object in the focal plane, i.e. a

thin optical section of the 3D plane [10]. A confocal laser scanning microscopy (CLSM) incorporates a laser to scan one pixel and one slice over an object.

Spine morphology is examined using stimulated emission depletion microscopy (STED) at the nanoscale during normal development in mice, and the hypothesis is tested that it is impaired in a mouse model of fragile X syndrome (FXS) [11]. Stimulated Emission Depletion (STED) microscopy overcomes the diffraction-limited resolution of a confocal microscope and creates an effectively smaller observation volume. Here two synchronized laser pulses are used to break the refraction barrier[12].

1.4 Mouse model to human model

Humans and mice share many common genetic features, and by examining a mouse's physiology, anatomy and metabolism, scientists can gain valuable insight into how humans function. Over the past century, the house mouse has become the preferred mammalian model for genetic research. At the sequence level, approximately half of the human genomic DNA can be aligned with mouse genomic DNA[13].

In the early days of biomedical research, scientists developed mouse models by selecting and breeding specific mice to produce offspring with certain desired characteristics. Now scientists use mice to simulate human genetic disorders to study their development and test new therapies. As a scientific tool, mice have helped speed up the research progress and enabled the development of important new drugs. Like the other Mammalians, mouse naturally has diseases that cause the degradation of their lifetime, including hypertension, cancer, diabetes and osteoporosis. However, certain diseases such as Cystic fibrosis and Alzheimer's affect humans but normally do not strike mice. For experimenting with these diseases in a mouse model, these diseases are induced in a mouse by manipulating the mouse genome and environment, i.e. the mouse is genetically engineered for that purpose [14].

1.5 Motivation

Extensive research has been done in the field of dendritic spine analysis. However, there is still scope for improvement. All those methods perform well to some extent, but in every case, much manual work must be done. Most existing methods involve serious manual intervention, which requires a lot of time and effort for the researchers to analyze a single spine. Therefore, we need an automatic method that minimizes user intervention and gives the desired result.

1.6 Scope of Current Work

The major focus of this thesis report is to provide loop detection in two-dimensional (2D) dendritic spine images of different time stamps of rat dissociated hippocampal cultures. Loop elimination is very important in a dendritic spine because two joint spines creating loops will not give correct results for feature extraction of spines like spine count, spine length etc. Three-dimensional (3D) microscopy is used for image acquisition since a 3D stack contains all pieces of information needed to reconstruct a focused 2D image. Maximum Intensity Projection (MIP) is often preferred to create a 2D image from a 3D stack as it retrieves the maximum intensity level along the z-axis for each x and y position. During image processing, MIP of the confocal z-stack is used to convert the 3D stack image into a 2D image. Gaussian de-noising is performed on a 2D MIP image for quality enhancement.

1.7 Organisation of the Thesis

In *Chapter 1,* the basic introduction of the dendritic spine is discussed and its importance in our memory generation and different pathological conditions. It is also discussed how the mouse model resembles with human model.

Chapter 2 is a brief survey of different work done to analyze the dendritic spine's shape and nature and how we get our motivation for work.

In *Chapter 3,* all the basic theoretical concepts related to the automatic Spine analysis, i.e. 3D to 2D transformation, binarization, distance transform, fuzzy distance transform, and skeletonization, are briefly discussed.

Chapter 4 discusses the basic requirement to eliminate loops and the main approach and algorithm to detect those loops in a dendritic spine analysis.

Chapter 5 explains developing the GUI for automatic 2D-Spine analysis using the basic QT GUI module. The steps to use the GUI are also included here.

Chapter 6 discusses the overall work related to its advantage, shortcomings, future scopes, and conclusion.

Chapter 2

Literature Survey

This survey mainly focuses on experimental work that has analyzed the nature and morphology of dendritic spines. The search for the mechanisms underlying learning in the brain spans more than a century. In 1888, Cajal first described the dendritic spines, which had been discovered using a silver-impregnation protocol developed by Golgi. In the earliest form of this debate, Cajal speculated that learning required novel neuronal growth (Ramon y Cajal 1893).

At the same time, recapitulating an earlier suggestion from Spencer (1862), Tanzi (1893) argued that changes in existing connections might underlie information storage in the brain. In 1973 it was discovered that brief tetanic stimulation produced a long-lasting form of synaptic plasticity, long-term potentiation (LTP), that can last for hours or days in the mammalian hippocampus (Bliss & Lømo 1973) [15].

Later in 1982, Hopfield nicely related LTP to neural network theories of brain function because it implements a local learning rule, an essential element for associative neuronal networks, and ensures many of the computational features that make neural networks so attractive [16].

2.1 Literature survey on the classification of spines:

In 1970 Peters and Kaiserman- Abram categorized the dendritic spines into three categories based on the relative sizes of the spine, head and neck [17]

1. Mushroom spines with a large head and a narrow neck.

2. Thin spines with a smaller head and a narrow neck.

3. Stubby spines without an obvious constriction between the head and the attachment to the shaft.

In 1974 Skoff and Hamburger added a further category, the so-called filopodium, named for their hair-like morphology, reminiscent of axonal filopodium [18].

In 2008 Lohmann and Bonhoeffer showed that filopodia frequently make contact with axons, some of the mares short-lived, and some of the mares selectively stabilized, depending on the axon type indicating that filopodia are capable of choosing between potential synaptic partners before a mature synapse is established [19].

2.2 Literature survey on the link between dendritic spines shapes and how it affects mental retardation:

A link between mental retardation and altered dendritic spines was suggested for the first time in 1974 (Purpura,1974). Purpura showed that mental retardation was associated with abnormally long, thin spines and an absence of short, thick spines on dendrites of cortical neurons in retarded children [20].

A. Alvarez *et al.* [21] review some spine detection and reconstruction methods and conclude that dendritic spines undergo changes in shape and size, and their turnover rates decline with age.

Hosokawa et al. [22] made a statistical analysis of changes in the length of individual spines using confocal microscopy. They used confocal microscopy of hippocampal slices in which a specially developed "DiI-microdrop technique stained individual CA1 pyramidal cells." Synaptic potentiation was induced by "chemical LTP," produced by applying a superfusion solution containing elevated Ca2+, reduced Mg2+, and tetraethyl ammonium. Using this experimental approach, the authors observed that a subpopulation of (small) spines extended, and they reported an increased range of angular displacement of spines in the potentiated tissue.

In 1992 Harris et al. showed that the number of spines nearly doubles from postnatal day 15 to adulthood. However, this doubling has not been observed uniformly across all spine subtypes: thin spines, mushroom spines containing perforated PSD and spine apparatuses, and branched spines increase by about four-fold, whereas other types decrease in numbers or do not change [23].

In addition, in 1999, Kirov and Harris showed that mature hippocampal neurons could produce new spines. Filopodia are rarely observed in the mature hippocampus. However, the inhibition of synaptic transmission in hippocampal slices triggers the outgrowth of filopodia and newly formed spines, possibly compensating for the loss of synaptic activity [24].

In 2014 Rafael Yuste [25] viewed the dendritic spine behaviour from the perspective of the circuit function and showed how the spine would endow these circuits to function as neural networks.

Roberto Araya [26] uses two-photon calcium imaging of neocortical pyramidal neurons of the mouse to analyze the correlation between the morphologies of the spine activated under minimal synaptic stimulation and the excitatory postsynaptic potential they generate. They show that spike-timing simulation can induce synaptic potential and selectively shorten the length of the spine neck.

2.3 Literature survey on automated tools invented for spine analysis:

W. Christopher Risher *et al.* [27] built a RECONSTRUCT software that successfully conveyed the maturational shift in spine types during mouse primary visual cortex development. They used the Golgi-cox staining protocol, acquired the image, and imported the z-stack into an image analysis program. Though it can be a powerful tool for studying neuronal ultrastructure, Golgi-Cox staining has several drawbacks. Perhaps the biggest hindrance to a wider acceptance

of this method is the time commitment involved. Another significant drawback to Golgi-Cox staining is the inherent differences in spine classification from analyst to analyst. Individuals can assign highly differing spine classifications even when analyzing the same dendrites. This subjectivity makes it difficult, if not impossible, to compare results from different analysts, which can be a significant concern for experiments with extremely large data sets that are to be analyzed by more than one individual.

In 2016 Basu *et al.* [28] proposed a semi-automated method named 2D-Span for quantitative analysis of spine morphological changes with reduced manual intervention. This tool is useful in various applications involving large-scale annotation of dendritic spines for quick and accurate assessment of spine plastic changes. They used the confocal microscopic image of dendritic spines from disassociated hippocampal cultures. For the spine analysis, the user must select a dendritic segment by marking the two points, automatically segmenting the spines using the designed convolution kernels, and finally mark the spines of interest to extract relevant features like length and head width of the spine with high accuracy and minimal intervention. This method counts the number of dendritic spikes along with the classification of four types of the segmented dendritic spine (Stubby, Mushroom, Filopodia and Spine-head Protrusion). This method allowed us to record noticeable changes in the area and length of dendritic spines, which are the two most important attributes of spine plasticity. 2dSpAn requires considerably less user involvement compared to the work by Ruszczycki et al. [29]. As a result, many spines can be annotated quickly and effortlessly without compromising the accuracy of the estimated spine features. This work depends on the user's selection of the interested dendritic region. Then a global binarization is performed over the image, which sometimes causes a noisy result and improper segments of interested spines.

Dr T. Worbs *et al.* [30] developed Imaris software for four-dimensional (4D) image analysis and automatic neuron tracing. Using Imaris for Neuroscientists, users can manage and organize

full experiments, including images and data analysis. The advantage of Imaris is the high-performance IMS file format which guarantees smooth navigation even in very large 3D datasets (TB range). The accuracy of the automated tracking was manually controlled, and only tracks with durations of >60 s were included in the analysis. Although Imaris is good for analysis of the overall spine, due to huge manual intervention, it fails to model the 3D morphology of individual spine.

Pheng Shi *et al.* [31] proposed novel semi-supervised learning (SSL) approach to determine the online morphological classification of dendritic spines. Dendritic spines are detected and segmented from dendrite based on wavelet transform in their approach. Then spine features are extracted, and SSL is applied. However, this method's overall performance depends on the features and segment selected by the neuro-biologist for training.

An algorithm for 3D reconstruction and identification of the dendritic spine was proposed by Janoos *et al.* [32]. It is based on the skeletonization approach. Firstly, they find the skeleton of the whole dendritic spine and then the longest centre line is considered a dendrite and the smaller ones are considered a spine. Although this approach robustly reconstructs dendritic spines in 3D, the time required to get the centre lines (skeleton) from 3D volume and the complex Image is very expensive.

In 2018 Basu *et al.* [33] [34] proposed a method for quantitative analysis of individual dendritic spine in 3D. They use three-dimensional segmentation of spines using the Multi-Scale Opening (MSO) [35] approach to determine the 3D morphometric features of individual spines for quantitative analysis of spine plasticity. They used confocal microscopy images of dendritic spines from dissociated hippocampal cultures and brain slices. Although their method did not calculate the spine density as it requires more time but still produced a good result.

2.4 Recent studies on dendritic spine morphology and their relationship between ages and mental states:

In 2019 Benjamin D. Boros and M. Greathouse visualized and digitally reconstructed the three-dimensional morphology of dendritic spines from the dorsolateral prefrontal cortex in cognitively normal individuals aged 40-94 years.

Linear models defined relationships between spines and age, Mini-Mental State Examination (MMSE), and Alzheimer's disease (AD) pathology. Similar to findings in other mammals, spine density correlated negatively with human ageing.The presence of AD pathology correlated with increased spine length, reduced thin spine head diameter, and increased filopodia density.

Their study reveals how spine morphology in the prefrontal cortex changes in human ageing and highlights key structural alterations in selective spine populations that may promote cognitively normal function despite harbouring the APOE ε4 allele or AD pathology.

Therefore, there is still scope for improvement in the performance of this tool, especially in the context of a better user interface and pre-processing steps [36].

N. Ofer and D R. Berger Analyzed ultrastructural reconstructions from mouse neocortical neurons with computer vision algorithms. They demonstrated that the vast majority of spine structures could be rigorously separated into heads and necks, enabling morphological measurements of spine necks. They used a database of spine morphological parameters to explore the potential existence of different spine classes. Their analysis revealed that postsynaptic density size was strongly correlated with the spine head volume, and their data revealed a lack of morphological subtypes of spines and indicated that the spine neck length and head volume must be independently regulated [37].

In 2020 L K Parajuli and M Koike reviewed studies that have been instrumental in determining the three-dimensional ultrastructure of synapses. With a particular focus on dendritic spine synapses in the rodent brain, they discussed various key studies that have highlighted the structural diversity of spines, the principles of their organization in the dendrites, and their presynaptic wiring patterns, and their activity-dependent structural remodelling [38].

In 2020, to determine the events that initiate synaptic alterations, C Ortiz-Sanz and A Gaminde-Blasco applied oligomeric Aβ to primary hippocampal neurons and an ex vivo model of organotypic hippocampal cultures from a mouse after targeted expression to allow high-resolution imaging and algorithm-based evaluation of spine changes.

In vivo, time-lapse imaging showed that the three spine types were relatively stable, although their stability significantly decreased after treatment with Aβ oligomers. Unexpectedly they observed that the density of total dendritic spines increased in organotypic hippocampal slices treated with Aβ compared to control cultures. Specifically, the fraction of stubby spines significantly increased while mushroom and thin spines remained unaltered [39].

In 2021 J Choi and Sang-Eun Lee proposed a unified visualization framework for an interactive 3D dendritic spine analysis system, DXplorer, that displays the 3D rendering of spines and plots the high-dimensional features extracted from the 3D mesh of spines. With this system, users can perform the clustering of spines interactively and explore and analyze dendritic spines based on high-dimensional features. They proposed a series of high-dimensional morphological features extracted from a 3D mesh of dendritic spines. In addition, an interactive machine learning classifier with visual exploration and user feedback using an interactive 3D mesh grid view ensures a more precise classification based on the spine phenotype [40].

In 2022 S J Kim and Y Woo discovered a new function of Rai14(Retinoic acid-induced protein 14), an F-actin binding protein, in dendritic spine dynamics. The F-actin within dendritic spines

regulates their dynamic formation and elimination. Rai14 is an F-actin-regulating protein with a membrane-shaping function. They showed that Rai14 is localized at the spine neck and regulates spine density and function. Heterozygous Rai14 knockout mice showed impaired learning and memory and depressive-like behaviour. They that Rai14-dependent regulation of dendritic spines may underlie the plastic changes of neuronal connections relevant to depressive-like behaviours [41].

Chapter 3

Image Pre-processing Modalities

Image pre-processing is the steps taken to format images before any inference uses them. This pre-processing may include image resizing, orientation, and colour adjustment. Pre-processing is required to clean image data for any model input. Identifying the correct pre-processing steps are most useful for increasing performance which requires a firm understanding of the problem and data collection. Here 3D image to 2D image conversion is one of the primary steps of image pre-processing.

3.1 3D to 2D Conversion

It is very much possible to reconstruct a focused 2D image, which can adequately represent all the information in the 3D stack. A 3D stack contains all pieces of information, and it is needed to reconstruct a focused 2D image. To create a 2D image from a 3D stack, a projection in the z-direction is often preferred as it contains the highest amount of information and does not need any interactive interface. Above 80 per cent of the biologist community use MIP to reduce a 3D stack into a single 2D image. MIP retrieves the maximum intensity level along the z-axis for each x and y position. The image of the 3D stack is called the index map, while the image of intensity values corresponding to that index map is called the projection. Gaussian de-noising is performed on a 2D MIP image for quality enhancement. MIP is widely adopted as it is the simplest method of z-projection, parameter-free, fast and straightforward to use as in the NIH Fiji/ImageJ software tool. Our dataset is generated by different imaging neurons from rat dissociated hippocampal cultures using a confocal light microscope before and after chemically induced long-term potentiation (cLTP).

❖ Image Pre-processing steps are given below :

- Steps to convert a 3D image to stack splitting:

i. Plugins→LSM toolbox→Open LSM (See Figure 3.1 and 3.2)

ii. Image→Stack->Tools→Stack splitter (See Figure 3.3 and 3.4)

iii. Sliced Image Save as→Tif (See Figure 3.5)

iv. Opening the saved Image with IrfanView Software (See Figure 3.6)

v. After converting the image to a grayscale image and adjusting the colour (See Figure 3.7)

❖ Screenshots for a 3D image to stack splitting using Fiji Software :

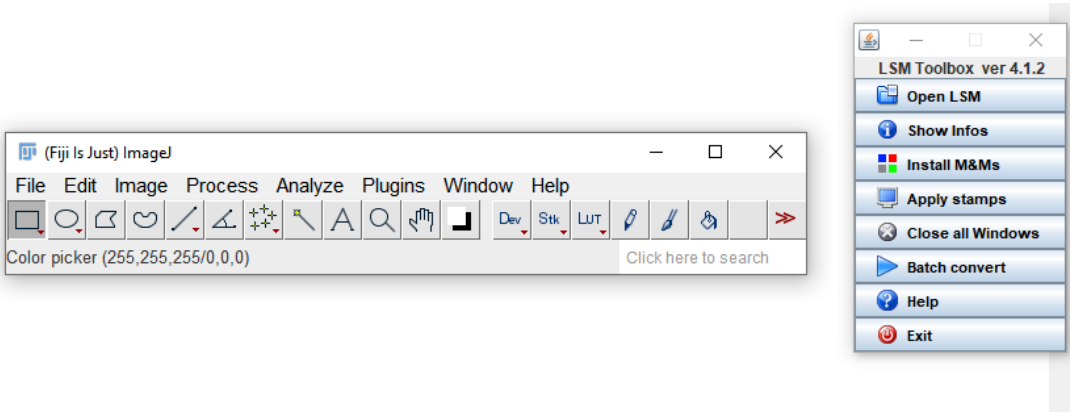

Figure 3.1. Open the LSM toolbox in Fiji(Refer to step i above)

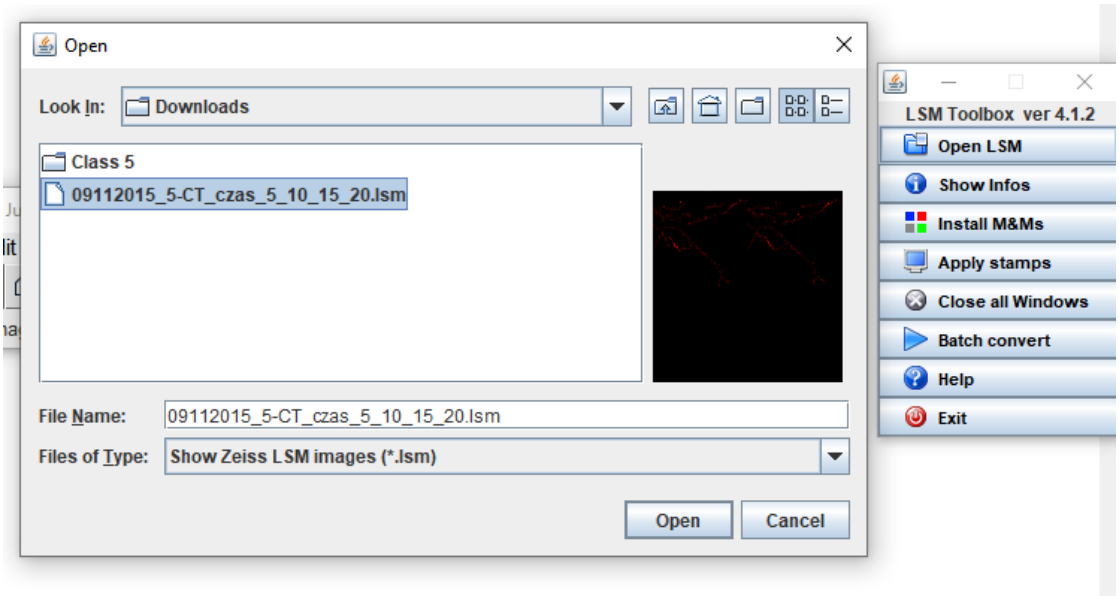

Figure 3.2. Open LSM image(Refer to step i above)

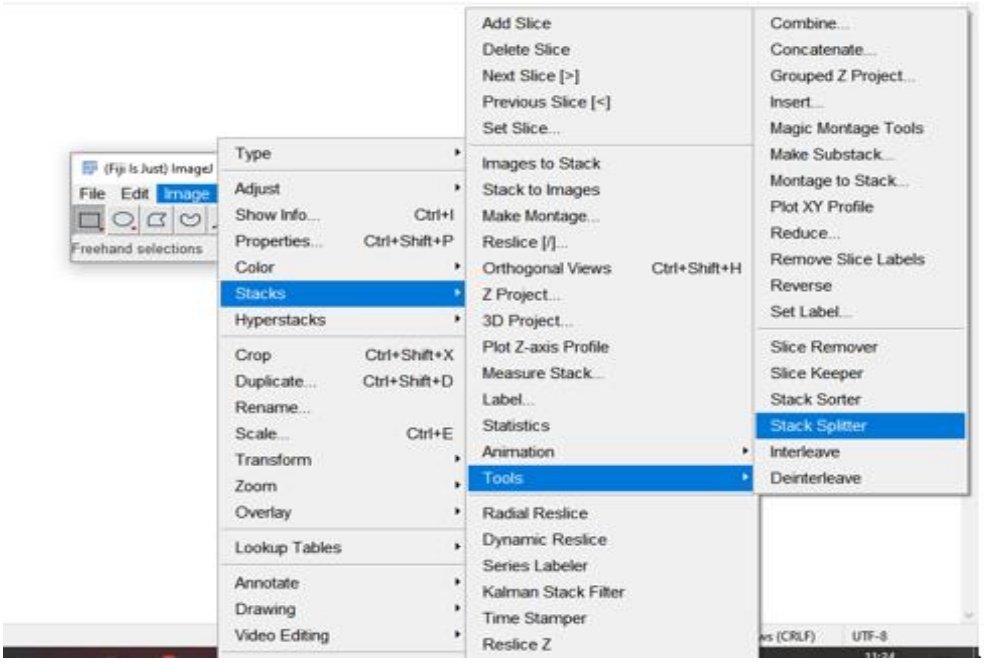

Figure 3.3.Navigate to stack splitter(Refer to step ii above)

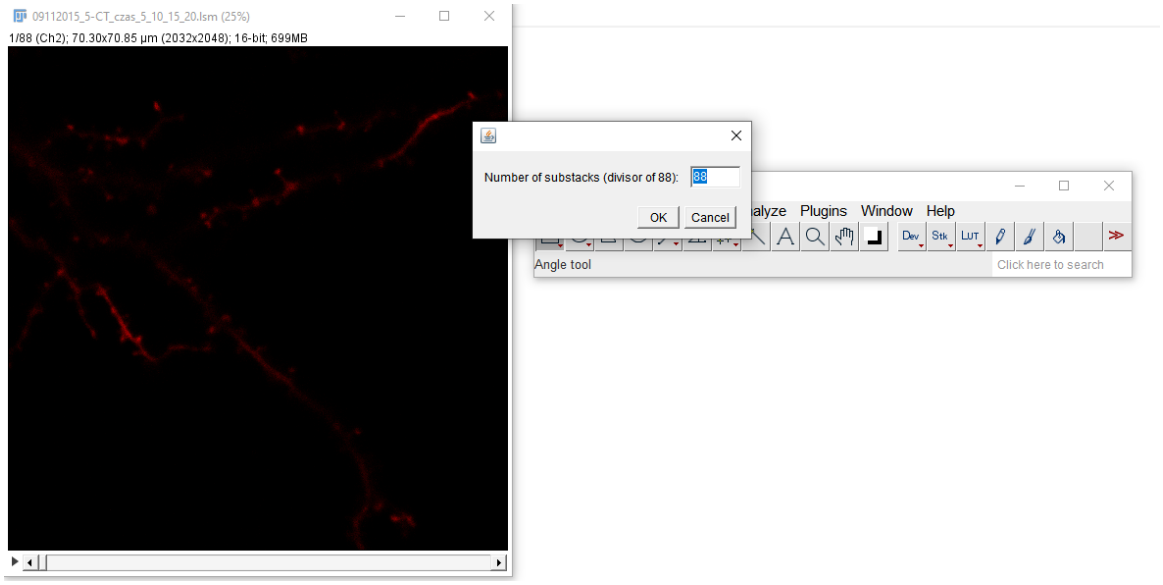

Figure 3.4. Stack splitting of a 3D image(Refer to step ii above)

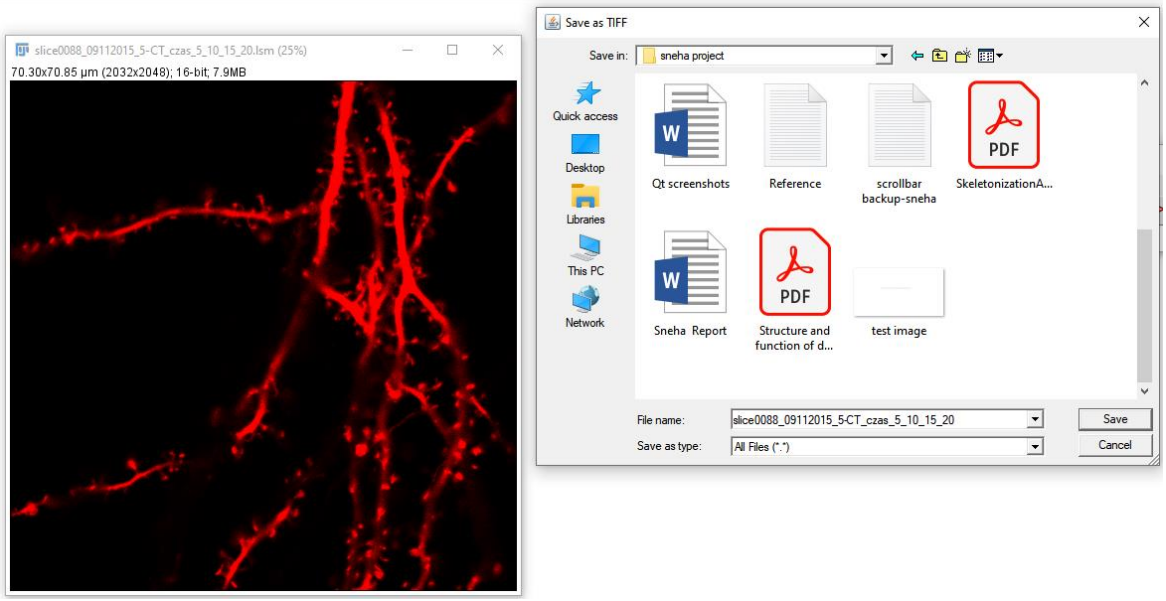

Figure 3.5. Saved sliced Image (Refer to step iii above)

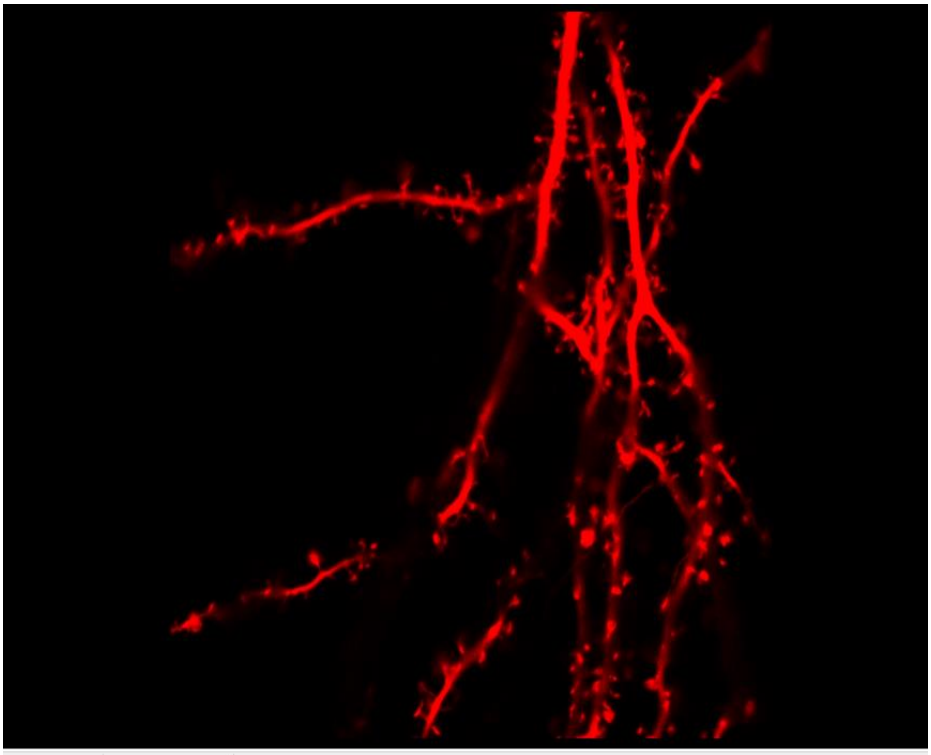

Figure 3.6. Open saved Image in IrfanView Sofware (Refer step iv above)

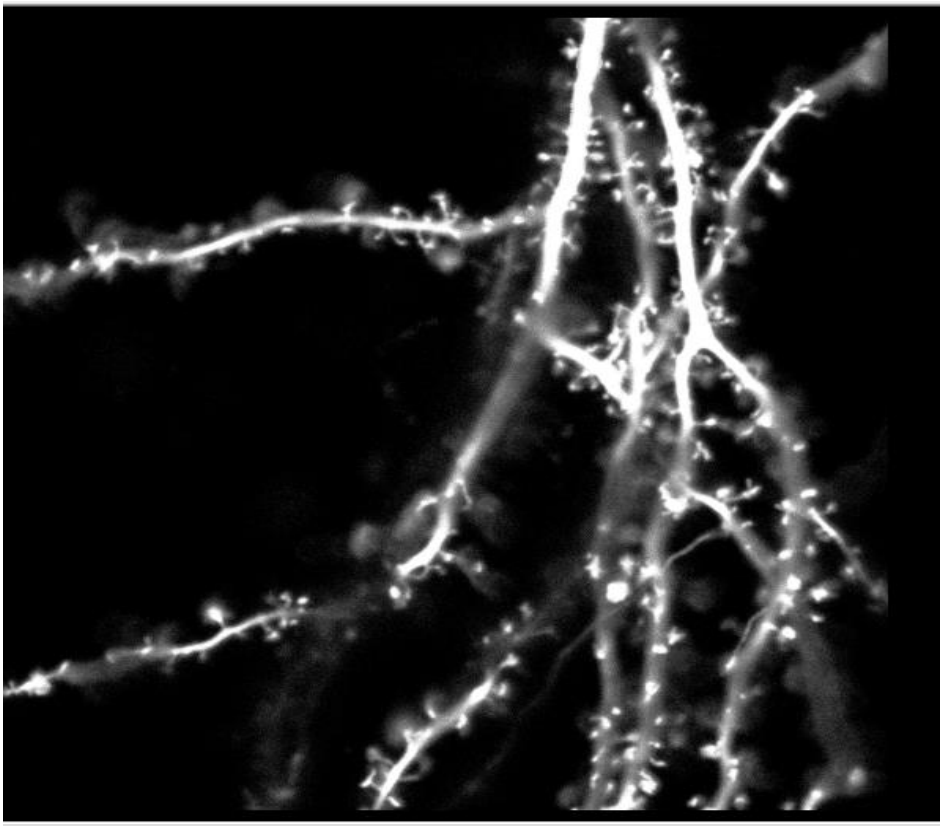

Figure 3.7. Converting the image to a grayscale image Refer to step v above)

- Steps for 3D to 2D image using the MIP concept:

  i. Process→Filter→3D Gaussian Blur 1.0 (See Figure 3.8)

  ii. Tif Image→Type→8 bit (See Figure 3.9)

  iii. Image→Stacks→Z project (See Figure 3.10)

  iv. Save Z-projection image (See Figure 3.11)

Figure 3.8. Applying Gaussian blur 3D filters (Refer to step i above)

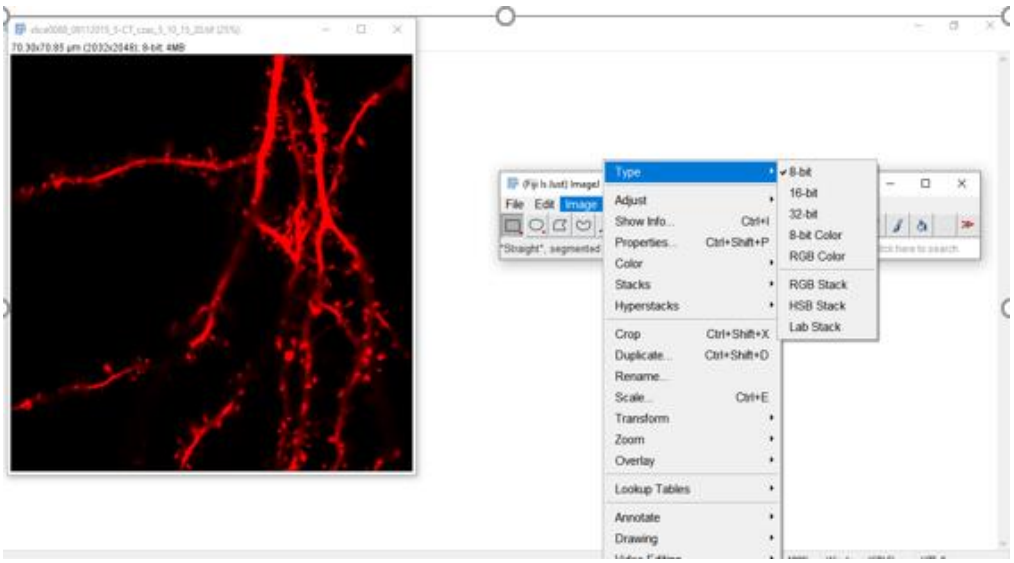

Figure 3.9. TIF image (Refer to step ii above)

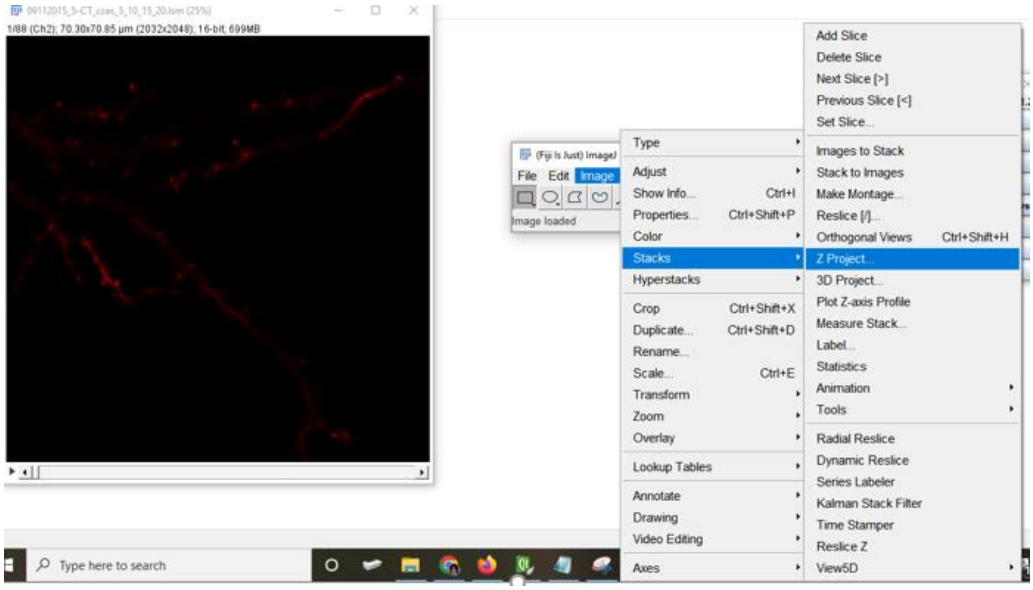

Figure 3.10. Applying Z-project (Refer to step iii above)

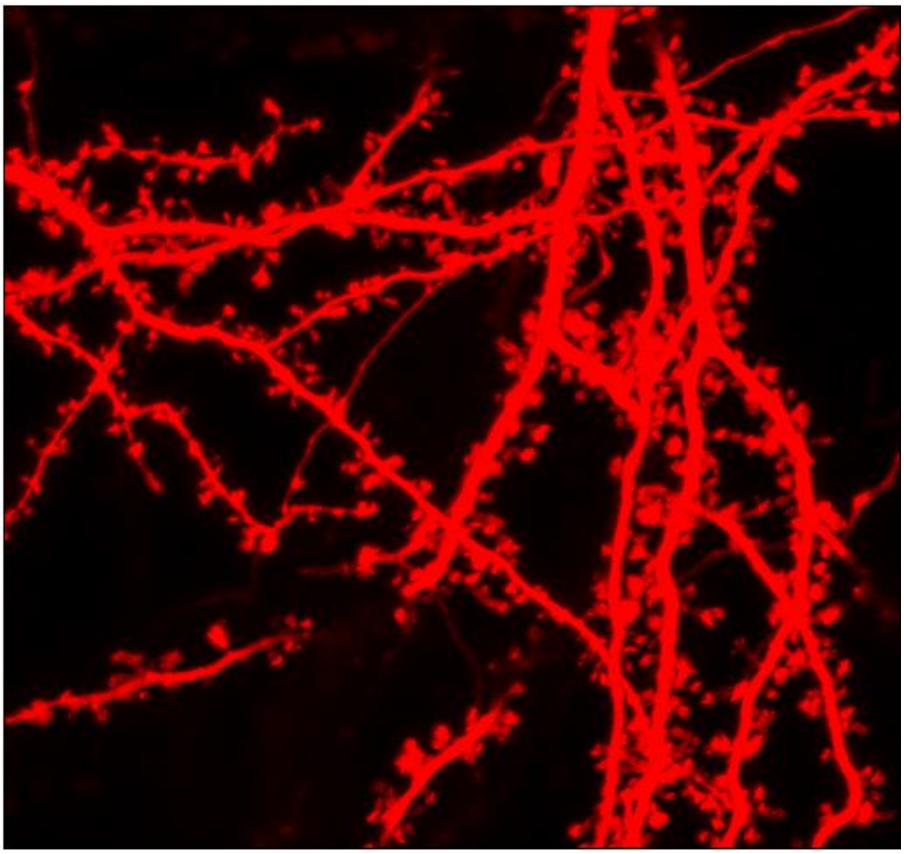

Figure 3.11.Image after MIP using Z-projection (Refer step iv above)

3.2 Binarization

Image Binarization is the pre-processing step for any image analysis and processing. Image Binarization is the Conversion of an image into a bi-level image. Image pixels are separated into a dual collection of pixels, i.e. black and white. It is a method to express a greyscale image in terms of 0 and 1. Therefore, only 1 bit is sufficient to represent one pixel. The simplest approach to binarization is thresholding. In thresholding, an optimal threshold value is chosen, and the pixels are classified as foreground or background by comparison with this threshold value.

Choosing an optimal threshold value for such documents is challenging [42]. Estimating the wrong threshold value results in the misclassification of the pixels [43]. This affects the results of binarization and the accuracy of pattern recognition applications.

Generally, binarization is categorized as Global and Local [44]. Global binarization is the technique in which a single threshold value is applied to binarize the entire image. It is a fast process but fails for the image with complex background.

The popular global thresholding method is Otsu's method, entropy-based thresholding. Global methods are useful when the intensity distribution of background and foreground pixels are very distinct. Some methods proposed for binarization consider adaptive local thresholding, which overcomes the drawbacks of global thresholding.

In the Local binarization technique, instead of a single threshold for the whole image, a different threshold value is chosen for every pixel. The threshold is chosen depending upon the neighbourhood pixels. Local thresholding does not give good results for the image suffering from background noise. Binarization techniques can also be categorized based on the threshold value criteria. Niblack [45] is a local thresholding method. Local thresholding methods calculate a different threshold value for each pixel. It uses the image's local statistics, such as variance and range, to calculate the threshold.

The most common way to convert a grey-level image into a binary image is to select a single threshold value, T. Then, all the grey values below T will be classified as black 0, i.e. background, and above T will be white, i.e. objects.

$$g(x,y) = 0 \ \ if \ f(x,y) < \ T$$
$$= 1 \quad if \ f(x,y) \geq T$$

In this approach global thresholding method is used for binarization. An Image histogram is determined, and the mean (M) and standard deviation (SD) are calculated. The threshold is calculated as follows:

$$Threshold = \frac{M + SD}{2}$$

And then the binarized value of pixel (i, j) is determined as:

$$If \quad pixel\,(i\,,j) \geq Threshold, \quad then \;\; pixel(i\,,j) = 1$$

$$Otherwise, \quad pixel(i\,,j) = 0$$

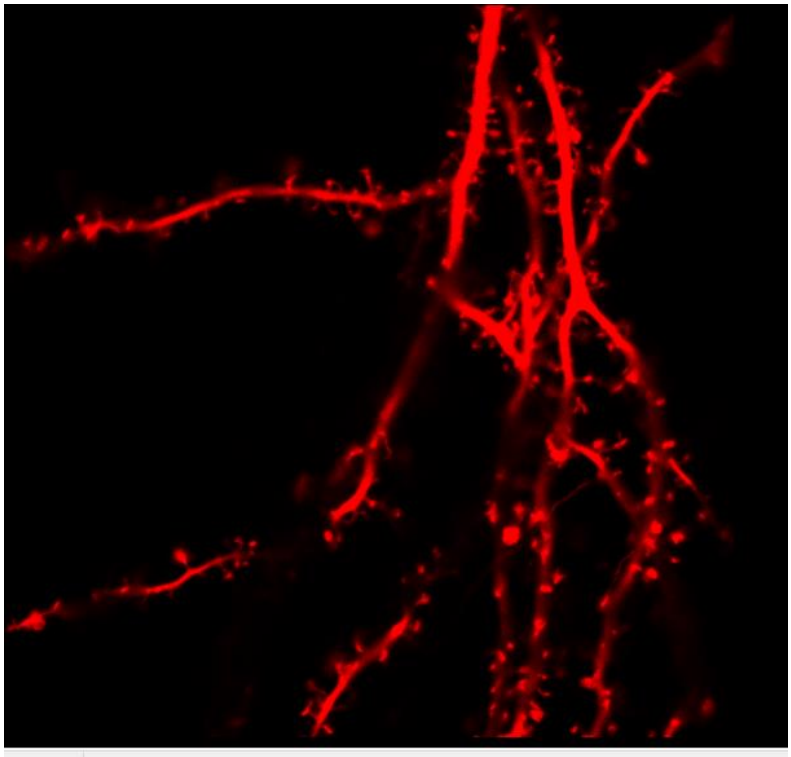

Figure 3.12.MIP image of a dendritic spine

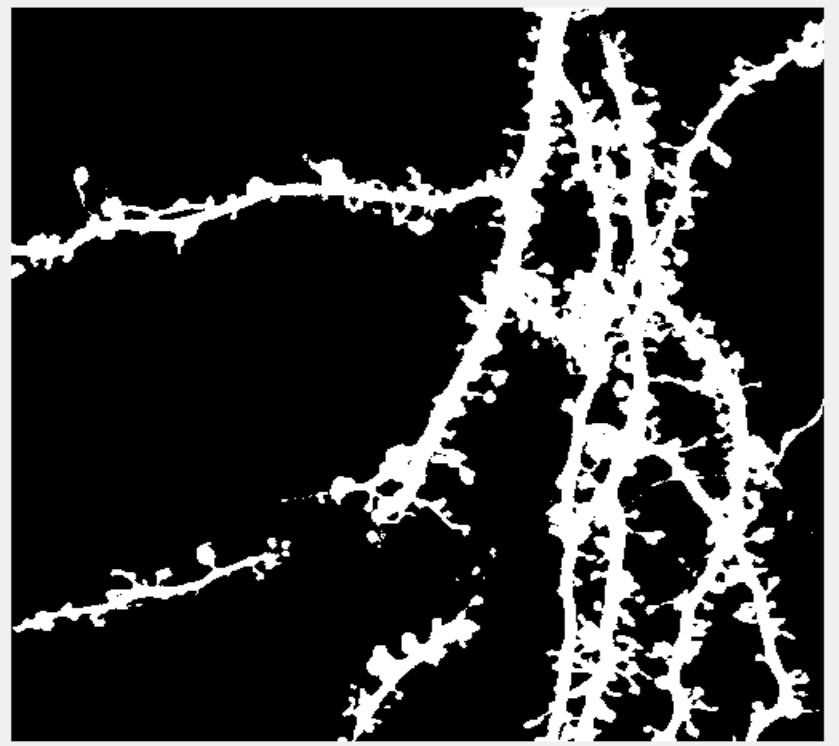

Figure 3.13. Binarized image of figure 3.12

3.3 Distance transform (DT/FDT)

A distance transformation (DT) is an operation that converts a binary picture consisting of feature and non-feature elements to a picture where each object pixel gets a value equal to the distance between itself and the nearest point in the background. Each background pixel gets a value equal to the distance between itself and the nearest point in an object. Therefore, in the resultant image, each element has a value that approximates the distance to the nearest feature element.

There are different DT methods proposed so far. The city block/chessboard distance family is the most popular one, called n-neighbour distance[46].

The city block distance metric measures the path between the pixels based on a 4-connected neighbourhood. Pixels whose edges touch are 1 unit apart; pixels diagonally touching are two units apart.

City block distance d_4 can be mathematically expressed as

$$d_4\big((x_1, y_1), (x_2, y_2)\big) = |x_1 - x_2| + |y_1 - y_2|$$

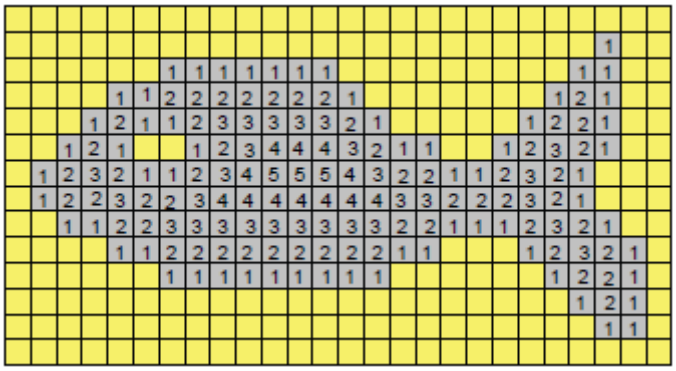

Figure 3.14.A Sample image of City block distance

The chessboard distance metric measures the path between the pixels based on an 8-connected neighbourhood. Pixels whose edges or corners touch are 1 unit apart.

Chess board distance d_8 can be mathematically expressed as

$$d_8\big((x_1, y_1), (x_2, y_2)\big) = max(|x_1 - x_2|, |y_1 - y_2|)$$

The Euclidean distance is the straight-line distance between two pixels.

Euclidean distance d_e between pixel (x_1, y_1) and (x_2, y_2) can be defined as,

$$d_e\big((x_1, y_1), (x_2, y_2)\big) = \sqrt{(x_1, y_1)^2 + (x_2, y_2)^2}$$

DT is widely applied in many applications, including the centre of maximal balls, Voronoi neighbourhood, DT-based interpolation, the multi-scale opening of conjoined structures and quantitative assessment of object morphology. In this method, DT is applied as a pre-processing step to skeletonization.

3.4 Skeletonization

Skeletonization is a process for reducing foreground regions in a binary image to a skeletal that largely preserves the extent and connectivity of the original region while throwing away most of the original foreground pixels. Analytically skeletonization is defined as a grassfire transformation [47] where the object is assumed to be a field of dry grass simultaneously lit at all boundary points. Centres of maximal balls (CMB) are used to define the quench points [48], which form the skeleton. We can imagine that the foreground regions in the input binary image are made of some uniform slow-burning material. Light fires simultaneously at all points along the boundary of this region, and watch the fire move into the interior. When the fire travelling from two different boundaries meets itself, the fire will extinguish itself and the points at which this happens form the so-called `quench line. This line is the skeleton.

The skeleton is useful because it provides a simple and compact representation of a shape that preserves many of the topological and size characteristics of the original shape. Thus, for instance, we can get a rough idea of the length of a shape by considering just the endpoints of the skeleton and finding the maximally separated pair of endpoints on the skeleton. Similarly, we can distinguish many qualitatively different shapes from one another based on how many `triple points' there are, *i.e.* points where at least three branches of the skeleton meet.

Skeletons are useful for object description, retrieval, manipulation, matching, registration, tracking, recognition, compression, and also, they facilitate efficient assessment of local object properties, e.g., scale, orientation, topology. Skeletonization has been widely applied in various medical imaging areas, including pulmonary, cardiac, mammographic, abdominal, retinal, and bone imaging.

A skeletonization algorithm generally consists of three major modules – primary skeletonization, final skeletonization, and pruning. The notion of primary and final

skeletonization was simultaneously introduced by Saha et al. [49], [50] and Arcelli and Sanniti di Baja [51]. Saha et al. described the two steps in a 3-D skeletonization algorithm using an iterative boundary erosion, while Arcelli and Sanniti di Baja presented the idea in 2-D using a DT-based method. Primary skeletonization produces a two-voxel thick "thin-set" [52] representing the medial axis of the object, where every voxel has at least one background neighbour (except at very busy intersections of surfaces and curves).

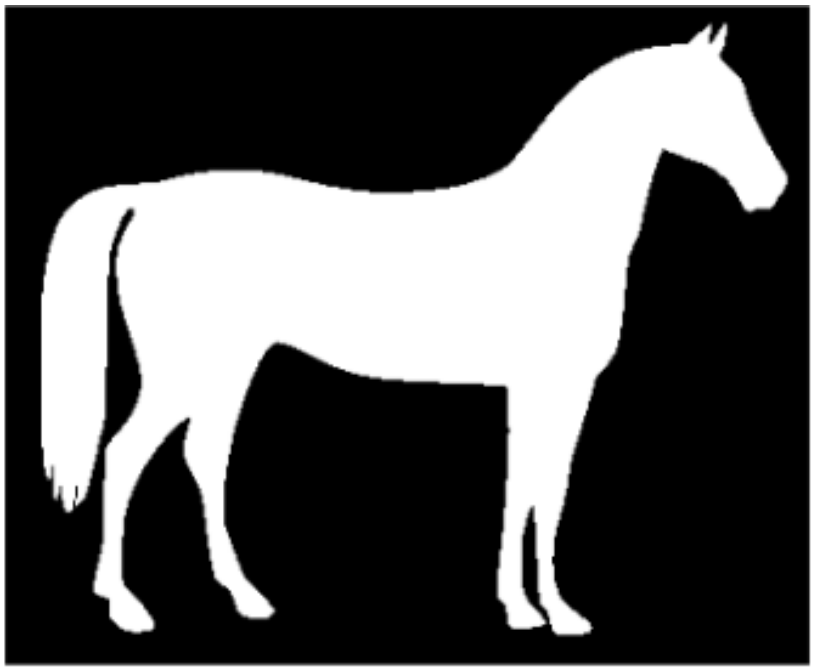

Figure 3.15. Original image of a horse

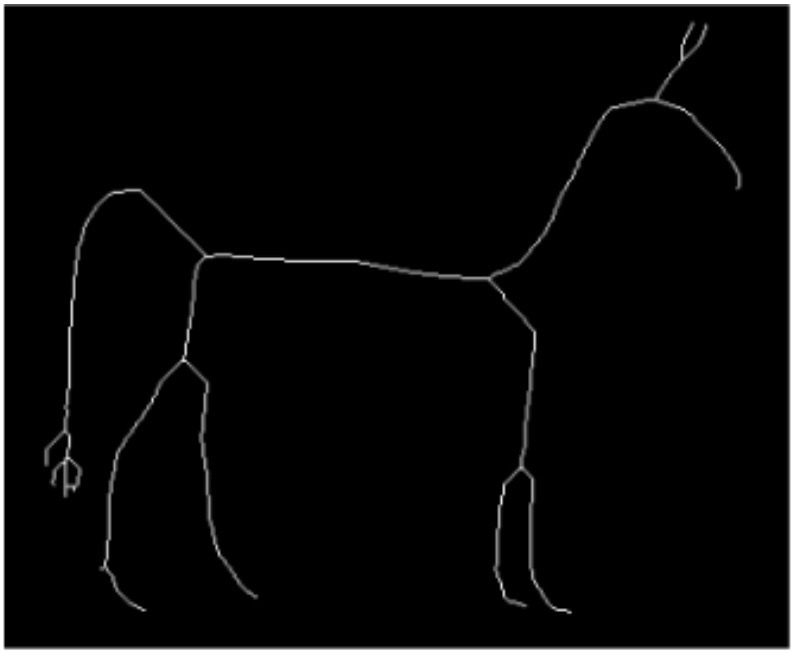

Figure 3.16. Skeletonization of a horse

(Image courtesy: Source image taken from website-

https://scikitimage.org/docs/stable/auto_examples/edges/plot_skeleton.html)

Chapter 4

Methodology

Loop detection in a dendritic spine image is very important to work in our 2D-SpAn-Automatic project. Sometimes it is observed that two spines are interconnected so that it only looks like a single spine. So, manually we can detect it as two spines, but in an automatic process, it would be counted as a single spine. This way, spine count or some spines in any 2D image will give us an incorrect result. First, we need to detect those loops, which should be eliminated later.

Loop detection in a dendritic spine:

Due to the Conversion of 3-D stack volume to 2-D using MIP, some information may be lost, affecting the algorithm's performance. Some loops may be created after pre-processing as binarization fails to differentiate two different spines in some regions where noisy pixels are present due to 3-D to 2-D Conversion. That is the reason eliminating the loop is necessary. To eliminate it, we need to detect the loop first. Here we followed one approach to detect loop or Cycle in a dendritic spine is discussed below.

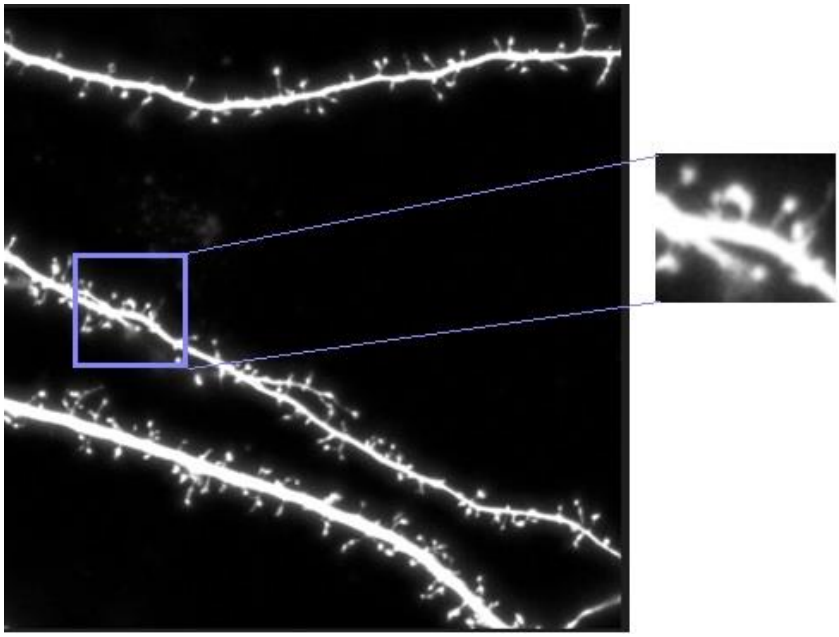

Figure 3.17. Loop detection in a dendritic spine image

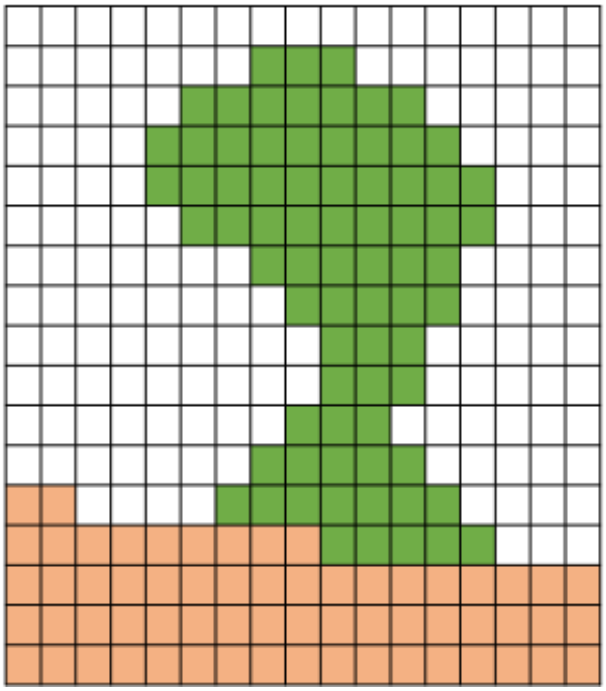

Figure 3.18. A sample image of a dendritic spine is shown in the 2D-Grid format.

Peach colour region represents a dendritic segment

Green region represents the spine

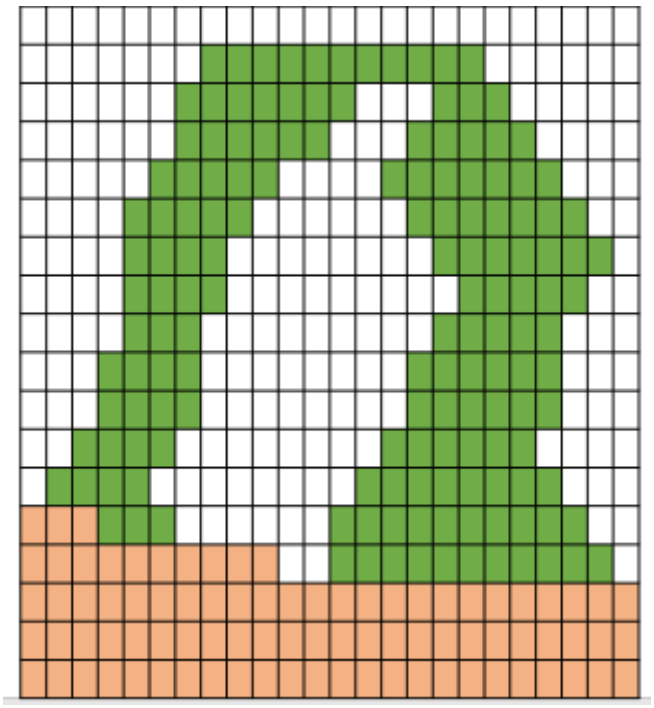

Figure 3.19. Two conjoined spines at the top create a loop presented in a 2D Grid format.

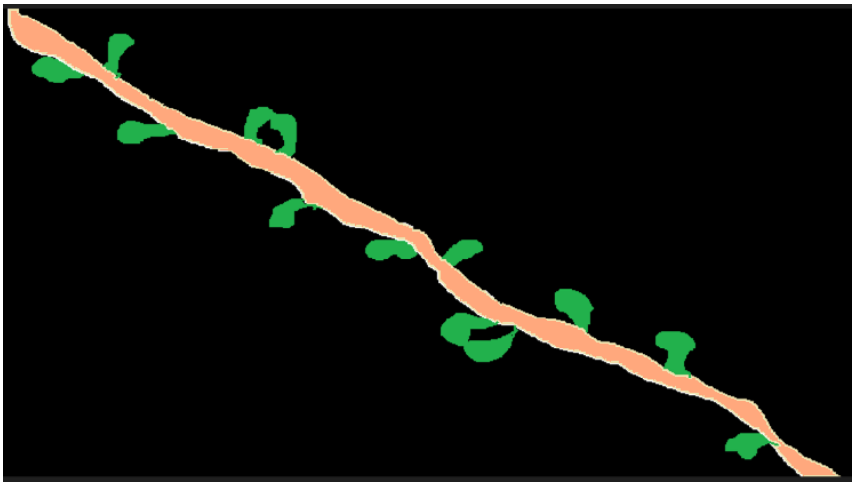

Figure 3.20. Morphological image of a loop in the dendritic spine

Algorithm 1. 2dSpAn loop detection algorithm in the dendritic spine.

Input : Read 2D_Image

Output : Boolean variable for loop detection 1 (Yes) or 0 (No).

Approach: Here, we consider the image a 2D grid with a 2D array 'arr' with r row and c column.

The idea is to use DFS (Depth First Search) Traversal on the image to detect a cycle

Algorithm Steps:

Here we consider the image a 2D grid with an r row and c column.

The idea is to use DFS Traversal on the image to detect a cycle. Below are the steps:

- Pick every pixel of the given image **((0, 0) to (r – 1, c – 1))** because there is no definite position of the Cycle.
- If a cycle exists, all the Cycle cells should have the same value and be connected. Also, check that the last and first elements form a loop (they should have different parents).
- A boolean variable that will store the result of the function **is Cycle ()**, which will be a **1** or **0**, respectively, indicating whether there is a cycle or not. If the function returns 1, then switch the ans variable to true, and break the loop else, continue.
- If the ans remains unmarked till the last, then print **No** otherwise, print **Yes**.

Pseudocode for this loop detection algorithm:

1. Load and read the 2D image.
2. Call the main driving function loopmain ( ).
3. In function, loopmain define the array and call the detectcycle (arr).
4. Taken an array visited. Initially, mark all the cells as unvisited. Take a boolean variable cycle to store the result.
5. As there is no fixed position of Cycle, we will have to check for every array. If Cycle is present and we have already detected it, then break this loop.
6. Take (-1, -1) as the source node's parent. If the cell is unvisited within a loop, call another function to check whether Cycle is present or not. If that function returns 1, we have encountered a cycle, then break the loop and print "Loop is present in spine analysis". Otherwise, a loop is not present.

Function **isCycle()** to check if cycle/loop is present or not

1. Mark the current vertex as true. Next, check within a loop to generate all possibilities of adjacent cells and check them one by one.
2. Check for all 4 neighbour directions, top, left, right and bottom. A cycle exists if an adjacent node is already marked as visited and not a parent node.
3. Set cycle variable to true.
4. Return true to iscycle() function.

Chapter 5

Introduction to 2DSpAn-Auto Software:

2dSpAn-auto is a software mainly used for segmentation, classification, and analysis of structural changes of hippocampal dendritic spines. The software uses confocal light microscopy images of dendritic spines from dissociated hippocampal cultures as valid input. This software is used to precisely describe the morphology of individual spines in real-time experiments and quantitative analysis of spine morphological changes. This software is designed using the QT GUI module and used programming language C++ in the QT platform.

5.1 Introduction to QT framework:

Qt is a cross-platform application development framework for desktop, embedded and mobile. It is not a programming language on its own. It is a framework written in C++. Qt is very easy to use, and users do not need high-level training to get used to Qt. The Qt GUI module provides classes for system integration, event handling, 2D graphics, basic imaging, fonts and text. Although Qt is one of the IDE for C++, one can integrate OpenCV, python with Qt if required. A pre-processor, the MOC (Meta-Object Compiler), is used to extend the C++ language with features like signals and slots. Before the compilation step, the MOC parses the source files written in Qt-extended C++ and generates standard-compliant C++ sources. Thus any standard-compliant C++ compiler like Clang, GCC, ICC, MinGW and MSVC can compile the framework itself and applications/libraries using it. For application developers writing user interfaces, Qt provides higher-level APIs, like Qt Quick, that is much more suitable than the enablers found in the Qt GUI module.

5.2 User Manual of 2DSpAn-Auto Software:

In this section, we introduce the GUI of 2DSPAN-Automatic. Figure 5.1 shows the GUI followed by the description of each item on the GUI.

Figure 5.1. GUI of 2D SpAn Automatic

Load Image: First, the user must load the image of interest by clicking this button. After clicking the File button Load 2D MIP option appears. They can choose and load an image file from the directory. Figure 5.2 shows how the Load Image button works.

Figure 5.2. Load image in 2D SpAn-Automatic

Check box **ZOOM**: The user can zoom in or zoom out at any point to get a closer view of the segment of interest after checking this. When the user checks the checkbox, the zoom-in or zoom-out function is activated. Then the user can change the value to zoom in or out to that scale. The figure shows how the zoom check box works.

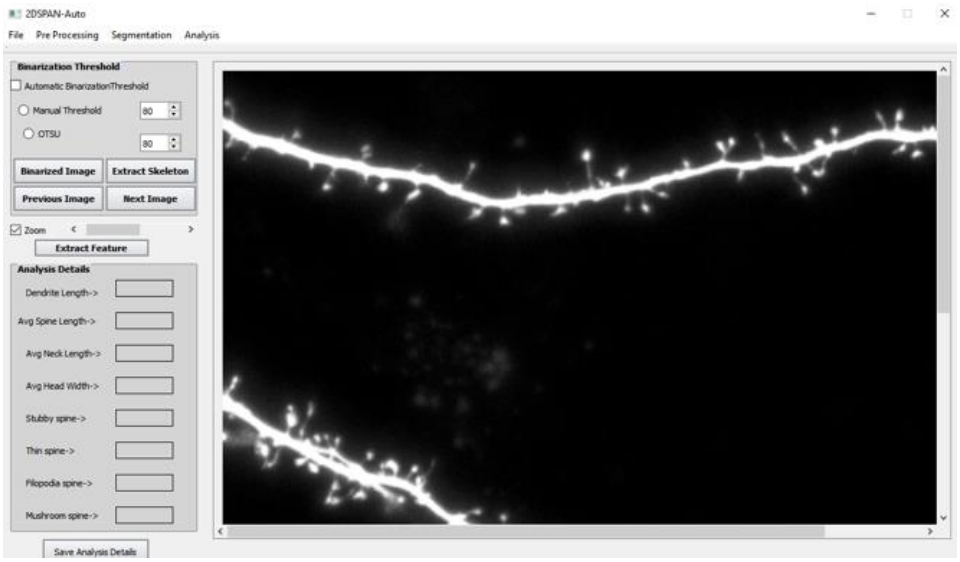

Figure 5.3. Check box ZOOM in 2D SpAn GUI

Binarized Image: To see the binary image user can click on the binarized Image button. The figure shows the binarized image.

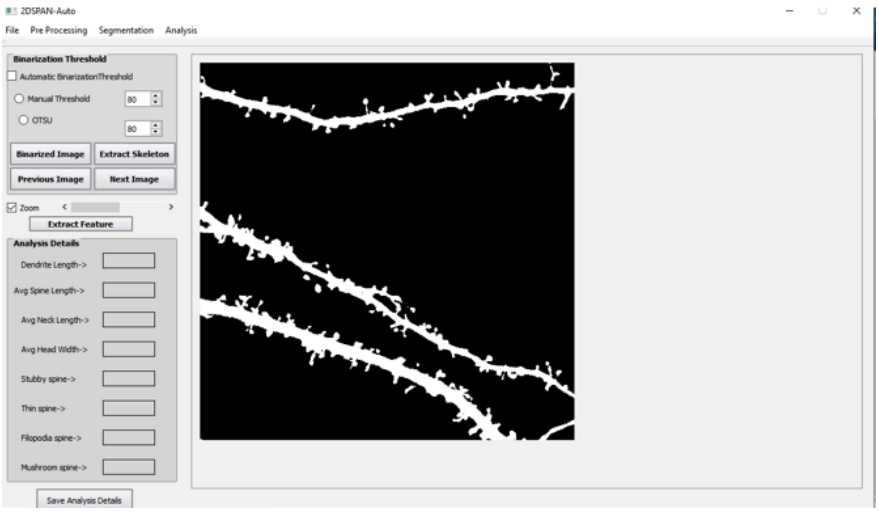

Figure5.4. Binarized Image option in 2D SpAn GUI

Skeleton Extraction: Dendrite extraction is one of the important steps of this method. As the name suggests in this step, we extract only the dendrite from the dendritic spine segment figure 5.5.

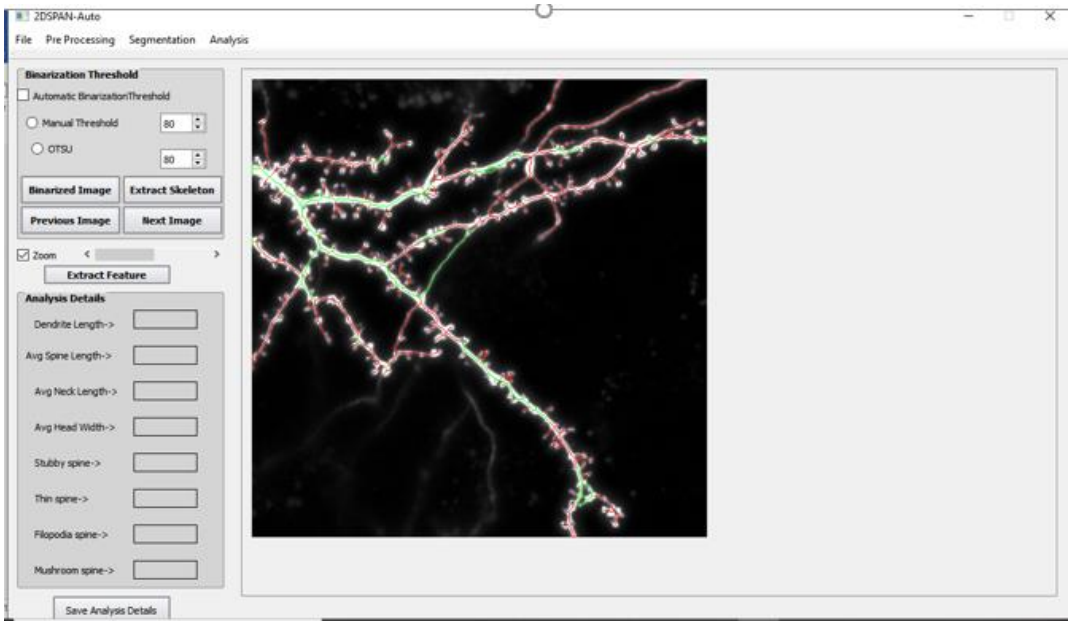

Figure 5.5.Extract Skeleton option in 2D SpAn GUI

Previous Image and Next Image:

To navigate directly from one image to the next or previous image, we can click the Next Image/Previous Image button.

Figure 5.6.Previous and next Image option in 2D SpAn GUI

Button **Extract Feature**: To extract the features from the 2D image user need to click this button. By doing so, this details analysis can be seen. Figure 5.6 shows how the Extract feature button works.

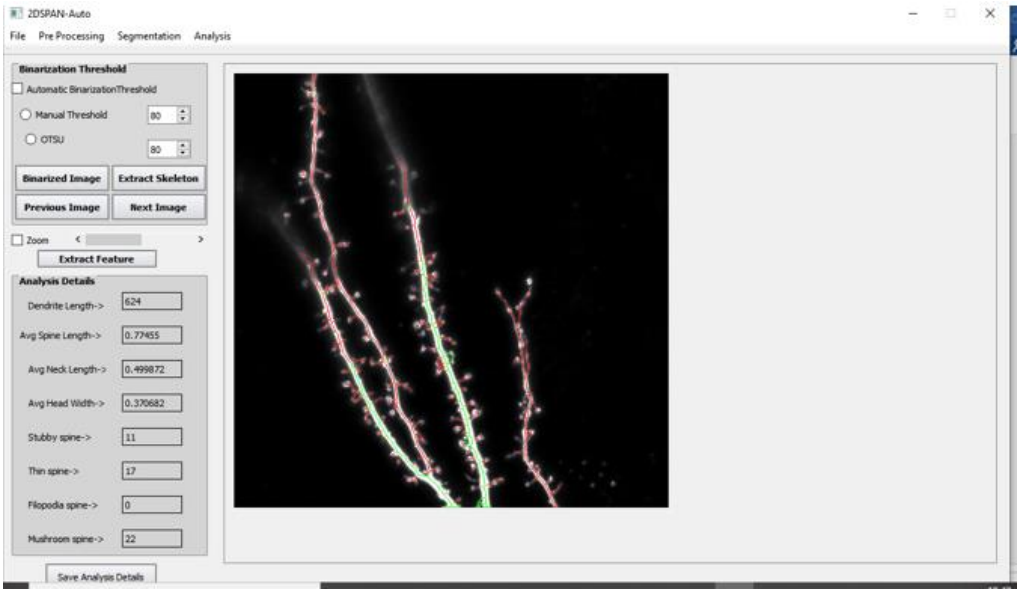

Figure 5.7.Extract Feature option in 2D SpAn GUI

Save Analysis Button: After extracting features to save the analysis in an excel sheet details, a user should click the button to save the analysis.

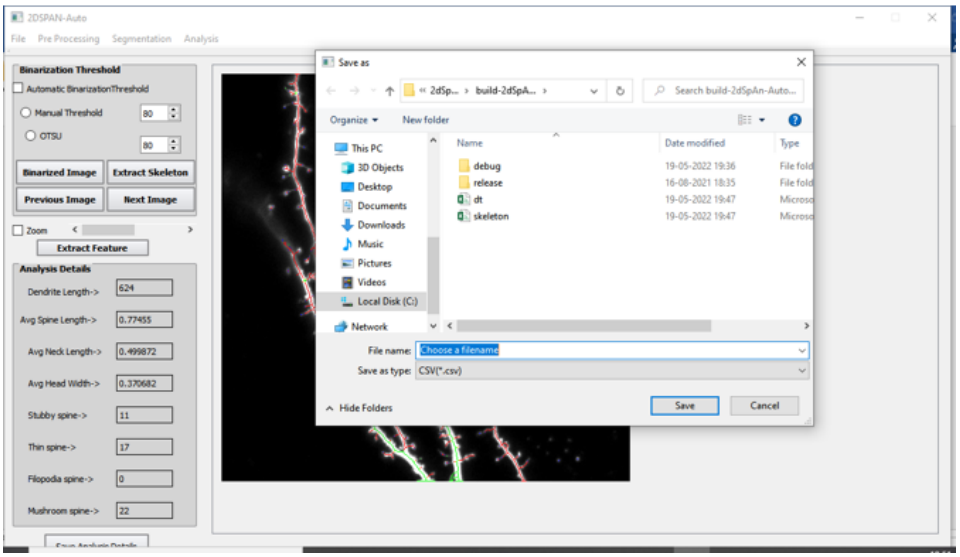

Figure 5.8. Save Analysis Button in 2D SpAn GUI

Chapter 6

Conclusion

This thesis introduces the theory and algorithm of loop detection in automatic spine analysis in 2-D MIP images. Initially, the skeleton of the dendritic spines is computed. Later, the spines are again imposed on the dendrite, and individual features are extracted during this. The total number of the spine, total dendrite length, and spine density were also computed. We review several methods of dendritic spine detection, reconstruction and analysis, along with a brief discussion on some of the digital topology applications that can be used for better performance of spine analysis methods. From this, we learned that many research works had been done so far in this area for 2D, 3D and 4D. However, still, there is a scope for improvement. These methods perform well to some extent, but in every case, much manual work must be done. Although the 2D-Span method required less human intervention, some tools still need manual point marking for selecting the region of interest. So, if human interaction is reduced, efficient results and proper analysis can be done. Our proposed method is completely automated and takes less time to analyze individual spine morphology.

Different experiment shows that during highly stressful or pathological conditions, spine dynamics unveil anomalies like loss or decrease in spine numbers, immature structure of spine, reduction of size, highly variable spine density, ectopic spine formation, and sometimes highly increased spine number. This method can be applied to determine the spine morphology and changes in spine density, number, and length in different stress models or pathological conditions like Alzheimer's, Schizophrenia and Fragile X-syndrome (FXS). This can be used in different neuro-biological studies.

This method is tested only on different MIP images of confocal light microscopy images of dendritic spines of rat dissociated hippocampal cultures. Due to the Conversion of 3D stack

volume to 2D using MIP, some information may be lost, affecting the algorithm's performance. Some loops may be created after pre-processing as binarization fails to differentiate two different spines in some regions where noisy pixels are present due to 3D to 2D Conversion.

Future work can be extended to automatic loop detection and removing the loop in 2D and 3D images. The whole dendritic spine can be reconstructed from the skeleton in 2D or 3D for better visualization.

References

[1] Papa, M., Bundman, M. C., Greenberger, V., & Segal, M. (1995). Morphological analysis of dendritic spine development in primary cultures of hippocampal neurons. *Journal of Neuroscience*, *15*(1), 1-11.

[2] Papa, M., & Segal, M. (1996). Morphological plasticity in dendritic spines of cultured hippocampal neurons. *Neuroscience*, *71*(4), 1005-1011.

[3] Kasai, H., Fukuda, M., Watanabe, S., Hayashi-Takagi, A., & Noguchi, J. (2010). Structural dynamics of dendritic spines in memory and cognition. *Trends in neurosciences*, *33*(3), 121-129.

[4] Kelley, B. J., & Petersen, R. C. (2007). Alzheimer's disease and mild cognitive impairment. *Neurologic clinics*, *25*(3), 577-609.

[5] Forrest, M. P., Parnell, E., & Penzes, P. (2018). Dendritic structural plasticity and neuropsychiatric disease. *Nature Reviews Neuroscience*, *19*(4), 215-234.

[6] Nikonenko, I., Jourdain, P., Alberi, S., Toni, N., & Muller, D. (2002). Activity- induced changes of spine morphology. *Hippocampus*, *12*(5), 585-591.

[7] Fiala, J. C., Spacek, J., & Harris, K. M. (2002). Dendritic spine pathology: cause or consequence of neurological disorders? *Brain research reviews*, *39*(1), 29-54.

[8] Hering, H., & Sheng, M. (2001). Dendritic spines: structure, dynamics and regulation. *Nature Reviews Neuroscience*, *2*(12), 880-888.

[9] Levet, F., Tønnesen, J., Nägerl, U. V., & Sibarita, J. B. (2020). SpineJ: A software tool for quantitative analysis of nanoscale spine morphology. *Methods*, *174*, 49-55.

[10] Pawley, J. B., & Centonze, V. E. (1994). *Practical laser-scanning confocal light microscopy: obtaining optimal performance from your instrument* (Vol. 2, pp. 44-64). Academic, San Diego, CA.

[11] Wijetunge, L. S., Angibaud, J., Frick, A., Kind, P. C., & Nägerl, U. V. (2014). Stimulated emission depletion (STED) microscopy reveals nanoscale defects in the developmental trajectory of dendritic spine morphogenesis in a mouse model of fragile X syndrome. *Journal of Neuroscience*, *34*(18), 6405-6412.

[12] Garini, Y., Vermolen, B. J., & Young, I. T. (2005). From micro to nano: recent advances in high-resolution microscopy. *Current opinion in biotechnology*, *16*(1), 3-12.

[13] Yue, F., Cheng, Y., Breschi, A., Vierstra, J., Wu, W., Ryba, T., ... & Ren, B. (2014). A comparative encyclopedia of DNA elements in the mouse genome. *Nature*, *515*(7527), 355-364.

[14] Vandamme, T. F. (2014). Use of rodents as models of human diseases. *Journal of Pharmacy & bioallied sciences*, *6*(1), 2.

[15] Bliss, T. V., & Lømo, T. (1973). Long- lasting potentiation of synaptic transmission in the dentate area of the anaesthetized rabbit following stimulation of the perforant path. *The Journal of physiology*, *232*(2), 331-356.

[16] Hopfield, J. J. (1982). Neural networks and physical systems with emergent collective computational abilities. *Proceedings of the national academy of sciences*, *79*(8), 2554-2558.

[17] Peters, A., & Kaiserman- Abramof, I. R. (1970). The small pyramidal neuron of the rat cerebral cortex. The perikaryon, dendrites and spines. *American Journal of Anatomy*, *127*(4), 321-355.

[18] Skoff, R. P., & Hamburger, V. (1974). Fine structure of dendritic and axonal growth cones in embryonic chick spinal cord. *Journal of Comparative Neurology*, *153*(2), 107-147.

[19] Lohmann, C., & Bonhoeffer, T. (2008). A role for local calcium signalling in rapid synaptic partner selection by dendritic filopodia. *Neuron*, *59*(2), 253-260.

[20] Purpura, D. P. (1974). Dendritic spine" dysgenesis" and mental retardation. *Science*, *186*(4169), 1126-1128.

[21] Alvarez, V. A., & Sabatini, B. L. (2007). Anatomical and physiological plasticity of dendritic spines. *Annual review of neuroscience*, *30*(1), 79-97.

[22] Hosokawa, T., Rusakov, D. A., Bliss, T. V., & Fine, A. (1995). Repeated confocal imaging of individual dendritic spines in the living hippocampal slice: evidence for changes in length and orientation associated with chemically induced LTP. *Journal of Neuroscience*, *15*(8), 5560-5573.

[23] Harris, K. M., Jensen, F. E., & Tsao, B. (1992). Three-dimensional structure of dendritic spines and synapses in rat hippocampus (CA1) at postnatal day 15 and adult ages: implications for the maturation of synaptic physiology and long-term potentiation [published erratum appears in J Neurosci 1992 Aug; 12 (8): following table of contents]. *Journal of Neuroscience*, *12*(7), 2685-2705.

[24] Kirov, S. A., & Harris, K. M. (1999). Dendrites are more spiny on mature hippocampal neurons when synapses are inactivated. *Nature Neuroscience*, *2*(10), 878-883.

[25] Yuste, R. (2011). Dendritic spines and distributed circuits. *Neuron*, *71*(5), 772-781.

[26] Araya, R., Vogels, T. P., & Yuste, R. (2014). Activity-dependent dendritic spine neck changes are correlated with synaptic strength. *Proceedings of the National Academy of Sciences*, *111*(28), E2895-E2904.

[27] Risher, W. C., Ustunkaya, T., Singh Alvarado, J., & Eroglu, C. (2014). Rapid Golgi analysis method for efficient and unbiased classification of dendritic spines. *PloS one*, *9*(9), e107591.

[28] Basu, S., Plewczynski, D., Saha, S., Roszkowska, M., Magnowska, M., Baczynska, E., & Wlodarczyk, J. (2016). 2dSpAn: semiautomated 2-d segmentation, classification and analysis of hippocampal dendritic spine plasticity. *Bioinformatics*, *32*(16), 2490-2498.

[29] Ruszczycki, B., Wlodarczyk, J., & Kaczmarek, L. (2014). *U.S. Patent Application No. 14/237,352*.

[30] Worbs, T., & Förster, R. (2007). 4D-Tracking with Imaris. *Bitpl.-Oxford Instruments*.

[31] Shi, P., Huang, Y., & Hong, J. (2014). Automated three-dimensional reconstruction and morphological analysis of dendritic spines based on semi-supervised learning. *Biomedical optics express*, *5*(5), 1541-1553.

[32] Janoos, F., Mosaliganti, K., Xu, X., Machiraju, R., Huang, K., & Wong, S. T. (2009). Robust 3D reconstruction and identification of dendritic spines from optical microscopy imaging. *Medical image analysis*, *13*(1), 167-179.

[33] Basu, S., Saha, P. K., Roszkowska, M., Magnowska, M., Baczynska, E., Das, N., ... & Wlodarczyk, J. (2018). Quantitative 3-D morphometric analysis of individual dendritic spines. *Scientific reports*, *8*(1), 1-13.

[34] Basu, S., Saha, P. K., Baczynska, E., Roszkowska, M., Magnowska, M., Das, N., ... & Wlodarczyk, J. (2018, March). Segmentation and assessment of structural plasticity of hippocampal dendritic spines from 3D confocal light microscopy. In *Medical Imaging 2018: Biomedical Applications in Molecular, Structural, and Functional Imaging* (Vol. 10578, pp. 91-99). SPIE.

[35] Basu, S., Hoffman, E., & Saha, P. K. (2015, September). Multi-scale opening–a new morphological operator. *International Conference on Image Analysis and Processing* (pp. 417-427). Springer, Cham.

[36] Boros, B. D., Greathouse, K. M., Gearing, M., & Herskowitz, J. H. (2019). Dendritic spine remodelling accompanies Alzheimer's disease pathology and genetic susceptibility in cognitively normal ageing. *Neurobiology of ageing*, *73*, 92-103.

[37] Ofer, N., Berger, D. R., Kasthuri, N., Lichtman, J. W., & Yuste, R. (2021). Ultrastructural analysis of dendritic spine necks reveals a continuum of spine morphologies. *Developmental neurobiology*, *81*(5), 746-757.

[38] Parajuli, L. K., & Koike, M. (2021). Three-dimensional structure of dendritic spines revealed by volume electron microscopy techniques. *Frontiers in Neuroanatomy*, *15*, 39.

[39] Ortiz-Sanz, C., Gaminde-Blasco, A., Valero, J., Bakota, L., Brandt, R., Zugaza, J. L., ... & Alberdi, E. (2020). Early effects of Aβ oligomers on dendritic spine dynamics and arborization in hippocampal neurons. *Frontiers in synaptic neuroscience*, *12*, 2.

[40] Choi, J., Lee, S. E., Lee, Y., Cho, E., Chang, S., & Jeong, W. K. (2021). DXplorer: a unified visualization framework for interactive dendritic spine analysis using 3D morphological features. *IEEE Transactions on Visualization and Computer Graphics*.

[41] Kim, S. J., Woo, Y., Kim, H. J., Goo, B. S., Nhung, T. T. M., Lee, S. A., ... & Park, S. K. (2022). Retinoic acid-induced protein 14 controls dendritic spine dynamics associated with depressive-like behaviours. *Elife*, *11*, e77755.

[42] Jiang, L., Chen, K., Yan, S., Zhou, Y., & Guan, H. (2009, December). Adaptive binarization for degraded document images. In *2009 International Conference on Information Engineering and Computer Science* (pp. 1-4). IEEE.

[43] Chaki, N., Saeed, K., & Shaikh, S. H. (2014). Exploring image binarization techniques studies in computational intelligence.

[44] KaurGill, T. (2014). Document Image Binarization Techniques-A Review. *International Journal of Computer Applications*, *98*(12), 1-4.

[45] Niblack, W. (1985). *An introduction to digital image processing*. Strandberg Publishing Company.

[46] Borgefors, G. (1984). Distance transformations in arbitrary dimensions. *Computer vision, graphics, and image processing*, *27*(3), 321-345.

[47] Blum, H., & Nagel, R. N. (1978). Shape description using weighted symmetric axis features. *Pattern recognition*, *10*(3), 167-180.
.
[48] Jin, D., & Saha, P. K. (2013, September). A new fuzzy skeletonization algorithm and its applications to medical imaging. In *International Conference on Image Analysis and Processing* (pp. 662-671). Springer, Berlin, Heidelberg.
.
[49] Saha, P. K., & Chaudhuri, B. B. (1994). Detection of 3-D simple points for topology-preserving transformations with application to thinning. *IEEE transactions on pattern analysis and machine intelligence*, *16*(10), 1028-1032.
.
[50] Saha, P. K., Chaudhuri, B. B., & Majumder, D. D. (1997). A new shape-preserving parallel thinning algorithm for 3D digital images. *Pattern recognition*, *30*(12), 1939-1955.

[51] di Baja, G. S. (1994). Well-shaped, stable, and reversible skeletons from the (3, 4)-distance transform. *Journal of visual communication and image representation*, *5*(1), 107-115.

[52] Arcelli, C., & Di Baja, G. S. (1985). A width-independent fast thinning algorithm. *IEEE Transactions on Pattern Analysis and Machine Intelligence*, (4), 463-474.